

Trigonometric Parallaxes of Central Stars of Planetary Nebulae

Hugh C. Harris¹, Conard C. Dahn, Blaise Canzian, Harry H. Guetter, S.K. Leggett², Stephen E. Levine, Christian B. Luginbuhl, Alice K.B. Monet, David G. Monet, Jeffrey R. Pier¹, Ronald C. Stone, Trudy Tilleman, Frederick J. Vrba, Richard L. Walker

*U.S. Naval Observatory, 10391 W. Naval Observatory Rd, Flagstaff, AZ 86001;
hch@nofs.navy.mil*

ABSTRACT

Trigonometric parallaxes of 16 nearby planetary nebulae are presented, including reduced errors for seven objects with previous initial results and results for six new objects. The median error in the parallax is 0.42 mas, and twelve nebulae have parallax errors less than 20 percent. The parallax for PHL932 is found here to be smaller than was measured by Hipparcos, and this peculiar object is discussed. Comparisons are made with other distance estimates. The distances determined from these parallaxes tend to be intermediate between some short distance estimates and other long estimates; they are somewhat smaller than estimated from spectra of the central stars. Proper motions and tangential velocities are presented. No astrometric perturbations from unresolved close companions are detected.

Subject headings: Astrometry — ISM: Planetary Nebulae: General — Stars: AGB and Post-AGB — Stars: Distances

1. INTRODUCTION

Distances of planetary nebulae continue to be quite uncertain despite the increased quality and quantity of data available in recent years. In part, the variety and complexity of

¹Guest observer, Kitt Peak National Observatory, National Optical Astronomy Observatories, operated by the Association of Universities for Research in Astronomy, Inc., under cooperative agreement with the National Science Foundation.

²Current address Gemini Observatory, 670 North A'ohoku Place, Hilo, HI 96720-2700

nebular structures seen in high resolution images suggest that some methods of determining distances incorporate simplifying assumptions that are not realistic. These methods may be affected by errors even when detailed models are made of each nebula.

Measuring trigonometric parallaxes of the central stars of planetary nebulae (CSPN) can, in principle, provide a check on other methods for at least the nearest nebulae. Until recently, however, planetary nebulae have eluded successful parallax measurements. The Yale Parallax Catalogue (van Altena et al. 1995) lists 24 CSPN with measured parallaxes, but only one (the central star of NGC 7293) has an error less than 8 mas³, so these measurements are not significant. The Hipparcos satellite targeted 19 CSPN. Unfortunately, the faintness of the stars – near Hipparcos’ magnitude limit – caused the results to have errors larger than the ± 1 mas typical for most Hipparcos parallaxes. When combined with the small parallaxes that most of these CSPN have, the results were disappointing; only four stars had an error less than 50% of the parallax (Acker et al. 1998; Pottasch & Acker 1998). (Below we remeasure one, and find a parallax smaller than the Hipparcos value by 2σ .) Therefore, Hipparcos results have not been relied upon for establishing a planetary nebula distance scale.

Using the advantages offered by cameras with CCD detectors (high signal/noise, high dynamic range, high quantum efficiency), the U.S. Naval Observatory began observing some CSPN for parallaxes in 1987. Initial results were reported at IAU Symposia 155 (Pier et al. 1993) and 180 (Harris et al. 1997). Continued observations now give greatly improved and expanded results that are the subject of this paper.

A parallax for one CSPN has been measured using the fine guidance sensors on Hubble Space Telescope (Benedict et al. 2003), and data are currently being obtained for three other CSPN. Distances using the expansion method are also being measured with HST and the VLA by Hajian (2006) and collaborators. One other ground-based parallax study of three PNe (Gutiérrez-Moreno et al. 1999) gave results with less precision than is desirable. A few CSPN have companions for which a spectroscopic distance estimate has been made (Ciardullo et al. 1999). Finally, spectroscopic analysis of the CSPN has given distance estimates (through determination of the gravity of the CSPN) for many nebulae (Napiwotzki 1999; Napiwotzki 2001), some of which are in common with this paper. In Section 2 we present our astrometry, photometry, and parallax results, and in Section 3 we compare our results with those of other methods.

³ The parallax of the central star of NGC 7293 was marginally detected in several studies. The best result, according to the Yale Catalogue, was 5 ± 5 mas (Dahn et al. 1973; Harrington & Dahn 1980). Below we obtain 4.6 ± 0.5 mas, demonstrating the improved precision that can now be achieved.

2. OBSERVATIONS

2.1. Astrometry

The USNO parallax program began using CCD detectors in 1985. The observing and data processing techniques are described by Monet et al. (1992) and Dahn et al. (2002). Originally, the detector used was a Texas Instruments 800×800 (TI800) CCD, and observations of nine PNe were begun in 1987 using this camera. In 1992, a larger format Tektronix 2048×2048 (Tek2048) CCD was put into use, and, in 1995, use of the smaller TI800 camera was discontinued. The much wider field of the Tek2048 CCD (11 arcminutes, compared with 3 arcminutes for the TI800 CCD) and the greater full well of the Tek2048 pixels (giving good signal-to-noise data over a greater dynamic range of bright and faint stars) are both advantageous for parallax work; they allow selection of better reference stars (more stars, more distant stars, and stars with a more symmetrical distribution around the parallax star) which is important in sparse fields. All observations have been made with a wide- R filter.

The precision of USNO parallax results has improved steadily during the 20 years of using CCD detectors (Harris et al. 2005), owing to a combination of improved data quality control and the accumulation of large numbers of CCD frames over many nights and observing epochs. The precision of parallaxes is now better than 0.5 mas routinely, and is better than typical parallaxes from Hipparcos by factors of 2–3. For stars like CSPN at distances of hundreds of parsecs, this improvement in precision is a crucial factor to obtain significant results for many objects. In fact, as a class, planetary nebulae are the most challenging objects observed at USNO for obtaining scientifically useful results.

The results of our astrometric data analysis are shown in Table 1. Parallaxes determined with the TI800 CCD have a median error in the relative parallax of 0.56 mas, while parallaxes determined with the Tek2048 CCD have a median error of 0.42 mas. (For three stars, observations are continuing, so the latter error is expected to drop further as more data are obtained.) Three PNe (A24, A29, and A31) were begun with the TI800 camera, but satisfactory results were not obtained before use of that camera was discontinued. All three have small parallaxes where high precision is essential for useful results. Two of these three have now been completed with the Tek2048 camera, while the third (A29) has been dropped from the program. Three objects have results from both cameras, and one has a further (but not yet final) parallax observed with HST (Benedict et al. 2003). These three provide a test for consistency, and provide one of the few available assessments for accuracy: for Sh2-216, PuWe1, and NGC 6853 results from the two cameras agree within 0.4σ , 0.8σ , and 1.9σ , respectively; for NGC 6853, the result from the TI800 and Tek2048 cameras differ from HST by 0.8σ and 2.5σ , respectively. The residuals for NGC 6853 also show a correlation

with seeing that indicates a problem with the images of the central star, such as might be caused by the known faint companion star (see notes below). While the problem with NGC 6853 is not presently understood for certain, overall this level of agreement between different cameras is good.

A correction for the finite distances of the reference stars must be applied to convert each observed relative parallax to absolute parallax. This correction is important for PNe with distances of several hundred pc, and becomes increasingly important as the error in the relative parallax drops. This correction is shown as $\Delta\pi$ in Table 1. It has been determined both from spectroscopy and photometry of the reference stars. The use of *BVI* photometry for determining the corrections is done for all USNO parallax fields, and is described by Dahn et al. (2006, in preparation). In addition, for the PNe in this paper, spectra of many reference stars and spectral classification standard stars were taken at Kitt Peak National Observatory (4-m telescope, R/C spectrograph, CCD camera, 7Å resolution) and at USNO (1-m telescope, fiber-fed bench spectrograph, CCD camera, 8Å resolution). From these spectra, the strengths of 17 spectral features (H lines, Ca K, G and CN bands, MgH, MgI, Na D, CaI, and several Fe features) were measured and were used to determine the spectral type and luminosity class of each star and to check for any peculiarities (e.g. binary star, metal-poor star, emission lines, etc.). Particularly in fields at low galactic latitude, where reddening can be large and very different from star to star, the combination of spectral indices with photometric data is helpful for determining a reliable correction to absolute parallax.

The combined data give an estimate of the reddening and distance of each reference star, and allow the rejection from the astrometric solutions of any nearby (or uncertain) reference stars. Finally, 4 to 8 reference stars have been used in the final solutions for the PNe observed with the TI800 camera, and from 4 to 32 stars for those observed with the Tek2048 camera. Note that for fields close to the galactic plane (particularly Sh2-216, and to a lesser extent NGC 6853), reddening is large enough to make the distance of each reference star more uncertain, adding to the error in $\Delta\pi$. For all fields, Table 1 shows that the reference stars are typically at distances of 1–2 kpc. At these distances, $\Delta\pi$ is fairly small and reasonably well-determined. The median error in $\Delta\pi$ (the important quantity for this correction) is 0.17 mas, whereas the median error in π_{rel} is 0.42 mas. Therefore, for most of these PNe, the error in $\Delta\pi$ contributes only a small amount to the final error in the absolute parallax. Note that the use of *faint* reference stars is an important factor in keeping this contribution to the total error small. With *faint* reference stars, the error in the observed relative parallax usually dominates the total error.

2.2. Photometry

Photometry with B , V , and I filters has been obtained for the CSPN in this paper and their reference stars with the USNO 1-m telescope during 1994-2005. Standard stars (Landolt 1992) were observed each night. The filters have passbands close to the standard Johnson (for B and V) and Cousins (for I) passbands, and small color terms were determined and applied each night for these very blue program stars. The error of a single observation is typically 0.03 in V and 0.03 in $B - V$ and $V - I$.

Results are shown in Table 2 for the central stars. For A74, Table 2 shows the star to be notably brighter and bluer than found by Ciardullo et al. (1999) using HST. For the remaining 8 stars in common, we find a small mean difference of 0.066 ± 0.014 brighter in V and 0.036 ± 0.016 redder in $V - I$ than found by Ciardullo et al. Nebular contamination should not be causing significant errors for our CCD photometry of these CSPN with large nebulae, nor for the HST photometry. More likely these differences may be related to transforming magnitudes from the HST filter system used by Ciardullo et al. to the Johnson/Cousins system used here.

2.3. Notes for individual central stars

NGC 6720 (Ring Nebula) – No additional data; result repeated from IAU Symp. 180.

NGC 6853 (Dumbbell Nebula) – Distances to reference stars are somewhat uncertain because of uncertain reddening along the line of sight beyond the nebula. Our results with two cameras differ from each other by 2σ . We see systematic residuals vs. seeing that might be caused by a close pair of stars. A star with $V \sim 18.7$ and $1''$ separation is reported (Ciardullo et al. 1999), and may be the cause of our correlation with seeing. As a result, the ground-based astrometry may be adversely affected by the nearby star. Therefore, we adopt a weighted mean of the two USNO determinations given in Table 1, but with an error estimate inflated to account for the possible interference: $\pi(\text{USNO}) = 3.17 \pm 0.47$ mas. (This error inflation is based on subjective review of various parallax solutions using different subsamples of data.) An initial result using Hubble Space Telescope (Benedict et al. 2003) is $\pi(\text{HST}) = 2.10 \pm 0.48$ mas, and one additional HST epoch is being obtained. For an overall best current parallax, we adopt the weighted mean of $\pi(\text{USNO})$ and $\pi(\text{HST})$ of 2.64 ± 0.33 mas.

NGC 7293 (Helix Nebula) – Result improved from IAU Symp. 180.

A7 – Result improved from IAU Symp. 180. A faint, red companion star at $0.9''$

separation is possibly a physical companion (Ciardullo et al. 1999).

A21 – No additional data; result repeated from IAU Symp. 180.

A24 – Result improved from IAU Symp. 180 with Tek2048 camera, and the earlier preliminary measurement is omitted here. A red companion star at $3.4''$ separation is not a physical companion (Ciardullo et al. 1999).

A29 – Result from IAU Symp. 180, 2.18 ± 1.30 mas, noted “Insufficient data” to obtain a reliable parallax, and star dropped from USNO program. Result from Gutiérrez-Moreno et al. (1999), 3.3 ± 1.2 mas. Weighted mean of these two measurements gives 2.8 ± 0.9 mas, but these results are not included in the remainder of this paper (see Sec. 3).

A31 – Result improved from IAU Symp. 180 with Tek2048 camera, and the earlier preliminary measurement is omitted here. A red companion star at $0.26''$ separation is likely to be a physical companion and, if so, implies a distance < 440 pc (Ciardullo et al. 1999); the parallax in Table 1 is 1.5σ smaller than implied by such a close upper limit to the distance.

A74 – No additional data; result repeated from IAU Symp. 180. A star at $3.5''$ separation with $V = 18.44$, $V - I = 1.04$ is too distant to be a physical companion. Photometric difference between this paper and Ciardullo et al. (1999) suggests real variability.

Sh2-216 – Result improved from IAU Symp. 180; results with two cameras agree well. Distances to reference stars are uncertain because of the large reddening along the line of sight beyond the nebula; however, the parallax of Sh2-216 is sufficiently large that this uncertainty is a small fraction of the total parallax.

PuWe1 – Result improved from IAU Symp. 180; results with two cameras agree well. A red companion star at $5''$ separation is itself a resolved pair, but probably not physical companions at the same distance as PuWe1 (Ciardullo et al. 1999).

DeHt5 – New result; observations continuing. We see systematic residuals vs. seeing that might be caused by a close pair of stars. Frew & Parker (2006) find nebula may be ionized ISM.

HDW4 – New result. Frew & Parker (2006) find nebula may be ionized ISM.

Ton320 – New result.

RE1738+665 – New result. Frew & Parker (2006) find nebula may be ionized ISM.

PHL932 – New USNO result; preliminary result due to data over a small epoch range (Table 1); observations continuing. The parallax from Hipparcos is 9.12 ± 2.79 mas, but the USNO parallax in Table 1 is smaller by 2σ . A weighted mean of the Hipparcos and USNO

results is 3.63 ± 0.61 mas; we use only the USNO results hereafter, as discussed in Sec. 3⁴. Several peculiarities, see discussion in Sec. 3.

PG1034+001 (WD1034+110) – New result; preliminary result due to data over a small epoch range (Table 1); observations continuing. Large nebula with a larger outer halo (Hewett et al. 2003; Rauch et al. 2004). Frew & Parker (2006) find nebula may be ionized ISM.

3. DISCUSSION

Resulting combined parallaxes from Table 1 (and one from the literature) and distances are shown in Table 3. In constructing Table 3, several other parallax determinations from the literature have been ignored. The goal of our program has been to reach parallax errors much smaller than 1 mas, both to determine accurate distances and absolute magnitudes and to minimize possible Lutz-Kelker-type biases and bias corrections discussed below. With this goal in mind, we have chosen to ignore all parallaxes with estimated errors greater than 1.0 mas^5 in an effort to keep the accuracy of the measurements close to the precision errors

⁴ The central star of PHL932 appears to have a firm 3σ parallax observed by Hipparcos (Acker et al. 1998), but is found here to have a parallax smaller by a factor of 2.7 (2.0σ). We have run numerous solutions of our data, varying the reference stars and the frames included in the solutions, and these experiments appear to rule out a parallax anywhere near the large Hipparcos value. Is the Hipparcos parallax just a 2σ event, or an outlier caused by a systematic or non-Gaussian error to be rejected? Emission from the nebula of PHL932 should not affect the the Hipparcos measurement (Acker et al. 1998). The Hipparcos error is typical for this star near the faint limit for Hipparcos: the Hipparcos and Tycho Catalogues (Vol. 1, Table 3.2.4) give a median $\sigma_\pi = 2.98$ mas for $H_p = 11 - 12$ and $\sigma_\pi = 4.35$ mas for $H_p > 12$ at $\beta < 10$ deg, so for PHL932 ($H_p = 12.03$), we expect $\sigma_\pi = 3.5$ mas. Only 0.5% of stars in the Hipparcos catalog are as faint as PHL932; the statistical properties of these faint stars and the accuracy of their parallaxes and error estimates are not as well known as the bulk of the brighter stars in the catalog. Of the 19 CSPN observed by Hipparcos, only two are fainter than PHL932, and they both have larger Hipparcos errors (as do some of the brighter CSPN). Five of the 19 have negative Hipparcos parallaxes, and one might use this distribution to try to access the accuracy of the parallax and error values, but doing so would be difficult without knowing more about their true parallaxes. A remote possibility is that an astrometric perturbation has affected the Hipparcos measurements, and perhaps the USNO measurements too in an opposite sense by chance; if so, it should be identifiable with an additional couple of years of data. At present, we do not understand what has caused the Hipparcos and USNO parallaxes to differ.

⁵ The omitted measurements include that for PHL932 from Hipparcos, 9.12 ± 2.79 mas (see discussion in Sec. 2.3), for A21 from Gutiérrez-Moreno et al. (1999), 1.9 ± 1.3 mas, and for NGC 7293 from Dahn et al. (1973), 5 ± 5 mas. Also omitted are the three measurements from our own CCD program with the TI800 camera from Harris et al. (1997) that were noted as “Insufficient data, preliminary result” (based on the

given in Table 3. Omitting these results is an arbitrary procedure, and undoubtedly omits some valid results, but including them with appropriate weights would not change the Table 3 averages much.

The precision of the parallax determinations for most objects in Table 3 is improved considerably from earlier results (Harris et al. 1997): two stars have a result that is greatly improved, five stars are somewhat improved, three stars have no additional data so are unchanged, one star has been dropped, plus an additional six stars have been added. Of the five stars from Harris et al. (1997) that had sufficient data to have a believable result in 1997 but have improved results now, one star (A7) has a parallax larger by 2σ , one star (PuWe1) has a parallax larger by 1σ , and the other three have parallaxes changed only slightly. In 1997, four stars had a parallax significant at 5σ or greater, now 12 stars have a parallax with this level of significance.

The last column in Table 3 gives the tangential velocity determined from the relative proper motion in Table 1 and the distance, uncorrected for solar motion. The median tangential velocity is 29 km s^{-1} , the extreme is 88 km s^{-1} , and only one star (PG1034+001) has a tangential velocity above 55 km s^{-1} . These values by themselves are consistent with all stars being thin disk stars. However, using the new distance in Table 3, PG1034+001 has a tangential velocity sufficiently high that it could be a member of the thin disk or the thick disk (see note below).

Table 3 includes our determination of $E(B - V)$ for the central star from our observed BVI_C , assuming $(B - V)_0 = -0.38$ and $(V - I)_0 = -0.45$, and the derived M_V . The results are consistent with most stars having $6.0 < M_V < 7.5$. Notable exceptions are the central stars of A24, HDW4, and RE1738+665, which appear to be fainter, and the central star of PHL932, which is much brighter (see below). Phillips (2005a) suggested that in evolved PNe with low radio surface brightness ($\log T_B$ in the range -0.5 to -4.0), most central stars have $\langle M_V \rangle = 7.05$ with a range ± 0.5 . There are 11 stars in Table 3 within the range of T_B , and they have $\langle M_V \rangle = 7.07$, in excellent agreement with Phillips. However, the range is 4.43 (PHL932) to 9.43 (HDW4). Of the 11 stars, four differ from 7.05 by 1 mag or more, so are well outside the range in which Phillips suggests that most stars lie. These outliers indicate the real range of M_V is closer to ± 2 than ± 0.5 mag. Therefore, assuming a constant M_V to determine distances would result in significant errors, at least for these 11 stars. However, considering the peculiarity of PHL932 (discussed below) and the possibility that HDW4 and

number of frames, the distribution of parallax factors, the quality of the reference stars, and the stability of the parallax solutions) for A24, $3.11 \pm 1.12 \text{ mas}$, for A29, $2.18 \pm 1.30 \text{ mas}$, and for A31, $4.75 \pm 1.61 \text{ mas}$. Subsequently A24 and A31 have been measured with the Tek2048 camera and appear in Tables 1 and 3.

RE1738+665 are not true PNe (noted in Sec. 2.3), most of the remainder of our sample do satisfy Phillips’ suggestions of nearly constant M_V with a small true dispersion. We may be able to determine the true dispersion in M_V from these data after the nature of the nebulae for these outliers is clarified.

In Table 4, a comparison is made between the distances determined here and those from several other discussions of PNe distances. (The comparison papers are selected as particular methods or as representative review papers, and are not intended to give a thorough discussion of the many distance scale determinations in the literature.) In general, we find larger distances than have been determined in some older studies (although PHL932 is an exception to this trend). For example, we have observed eight of the 11 stars listed by Terzian (1993, his Table 3) as having distances < 300 pc. Terzian’s summary of nearby planetary nebulae was written prior to the availability of any useful parallax data. We find only two of these eight stars to be within 300 pc, while we find DeHt5 to be at a distance of 300 pc compared to Terzian’s 400 pc. The comparison is shown in Figure 1. Overall, the nearby PNe are not as nearby as believed by Terzian (1993). A comparison with Pottasch (1996) is shown in Figure 2, and this agreement is better. However, he included the preliminary parallax results for seven stars available then (Harris et al. 1997), so some improved agreement is expected.

Table 4 includes comparison with the statistical distances found by Cahn et al. (1992) (known to give “short” distances) and by van de Steene & Zijlstra (1994) and Zhang (1995) (both know to give “long” distances). Inspection of Table 4 shows that this paper gives distances that agree better with the short scale for some objects and better with the long scale for others; overall this paper gives an intermediate distance scale. However, the scatter in these comparisons with all three sources is large. With the large scatter, the small sample of objects in common makes quantitative comparisons uncertain. Furthermore, the poor performance of these statistical distances for evolved, low surface-brightness nebulae has been noted before (e.g. Ciardullo et al. 1999; Phillips 2005a; 2005b), as has the dichotomy between the short and long distance scales. Unfortunately, parallax measurements are necessarily confined to nearby distances where only evolved nebulae have been found, so our sample includes none of the young, high surface-brightness nebulae for which the statistical distance procedures probably give more reliable results. Therefore, a quantitative comparison between the parallax and statistical distances may be misleading when applied only to these evolved nebulae.

A comparison between spectroscopic distances (from analysis of the CSPN with non-LTE model atmospheres) and distances determined by trigonometric parallax was done by Napiwotzki (2001). He showed that spectroscopic distances were greater than trigonometric distances by a factor of 1.55, and he argued that a bias in the trigonometric distances

from a combination of sample selection and a Lutz & Kelker (1973) bias accounted for the discrepancy. Therefore, he concluded, the parallaxes corrected for his estimate of the bias supported the longer spectroscopic distance scale. Is this comparison still valid? First, Napiwotzki included the parallax of the central star of PHL932 from Hipparcos, and this paper finds the parallax to be smaller by a factor of 2.7. The remaining seven stars used by Napiwotzki, using parallaxes from Harris et al. (1997), have spectroscopic distances greater by a factor of 1.4. The new parallax values given in Table 3 have not changed much, but the errors are reduced, as noted above. We can now add four stars with new parallaxes and previous spectroscopic distances (Napiwotzki 2001; Napiwotzki 1999; Pottasch 1996; Werner et al. 1995). The comparison is shown in Figure 3. Three stars have a spectroscopic distance smaller than the distance determined by parallax, one star has good agreement, and 11 stars have a larger spectroscopic distance. The weighted mean distance ratio, using the error estimates for both distances, has spectroscopic distances larger than trigonometric distances by a factor of 1.3.

Napiwotzki (2001) used Monte Carlo models to estimate the bias in the parallax-based distances. A correction for the bias is significant when the parallax errors are an appreciable fraction of the parallax values, but it becomes small or insignificant when the parallax errors are reduced, as Napiwotzki’s Figure 2 illustrates. Several of the stars had small parallax errors then, and a bias correction would not have accounted for the discrepancy with spectroscopic distances. Now, with parallax errors reduced, a bias correction is also reduced. As Figure 3 shows, five central stars (NGC 7293, A31, Sh2-216, PuWe1, and DeHt5) have spectroscopic distances larger than the distances determined by parallax by more than 1σ in both errors *and* have small parallax errors; the mean σ/π is 0.12 for these five stars. The parallax data suggest these stars may have their spectroscopic distances overestimated.

An estimate for bias in the distances and absolute magnitudes derived from parallax measurements can best be made using Monte Carlo models like those of Napiwotzki (2001) or Smith (2003), for example. In many applications, models like these can quantify the effects of the Lutz-Kelker bias as well as additional effects from sample selection, and they can include a non-uniform space distribution of the observed objects. However, the sample of CSPN in this paper is not easily modeled because of the poorly defined criteria for selecting objects for our observing program. We have tended to include objects believed (from literature estimates) to be nearby, but the unreliability of these prior distance estimates has resulted in a few objects like A7 and A74 turning out to be at much greater distances than originally expected. Because all our parallax results have been published, there is no selection based on minimum parallax or maximum fractional error such as often occurs when extracting a sample from a large catalog of parallax results. A faint magnitude limit is not significant, because we routinely include fainter stars in our program, so magnitude and reddening

can be omitted from the model. We have rejected a few bright CSPN (where the CSPN has a brighter companion) from our program thus far, but this selection will not introduce significant bias.

As an indicator of the approximate bias in the results in Table 3, Figure 4 shows two models of a disk population of objects with a scale height of 250 pc and with parallax measurements with rms errors of 0.42 mas to match the errors in Table 3. In the models, 200,000 objects are placed with random positions, including the exponential scale height in z , in a box 3 kpc on a side with the sun at the center. (Fewer objects are plotted in Fig. 4 for clarity in the plot.) The model in the top panel has parallax objects selected randomly. The reduced density of objects in the upper right corner is due to incompleteness beyond 1.5 kpc caused by the box size. The top panel shows that the bias (a Lutz-Kelker-type bias, but modified by the non-uniform density of the disk distribution) causes the parallax distances to be underestimated by 19% (and the absolute magnitudes to be 0.38 mag too faint) for objects with estimated parallax errors of 20% of the measured parallax. In contrast, the model in the lower panel has an added selection of likely-nearby objects, attempting to match our sample selection. Objects were included in this model sample if their estimated distance was < 550 pc after adding a 30% rms error to the true model distance. (That is, a gaussian error was added to their true model distance to give a pseudo-distance, to mimic the rough estimated distances available from the literature for selecting objects to include in our program. Then, if this pseudo-distance was < 550 pc, the object was included in the model sample. These parameters were chosen to give a model sample with a median measured parallax of 2.54 mas and a median relative parallax error of 17%, values that closely match the actual parallax sample in Table 3.) The lower panel shows that the bias causes the parallax distances to be underestimated by 5% (and the absolute magnitudes to be 0.11 mag too faint) for objects with relative parallax errors of 12%, and the bias then drops to about zero for objects with relative parallax errors of 20%. With 12 objects in Table 3 having a parallax error less than 20% of the parallax, Fig. 4 suggests that the mean bias in their distances is probably about 5% or less.

The distance of PG1034+001 of 211_{-22}^{+26} pc is greater than the previous spectroscopic determination of 155 ± 50 pc (Werner et al. 1995). This has two ramifications for the discussion about the size of the PN and the galactic orbit of the central star (Rauch et al. 2004). First, the inner nebula with a diameter of 2 degrees has a linear diameter of 7 pc, the fainter halo with a diameter of 6x9 degrees has a diameter of 21x32 pc, and the outermost fragmentary shell has a diameter even larger. This nebula would be the largest known if it is a true PN. Its large size and a difference in radial velocity between the nebula and the central star has led to debate about the origin of the nebulosity (Chu et al. 2004; Frew & Parker 2006). However, some interaction with surrounding interstellar material is expected for large, old,

evolved PNe (Tweedy & Kwitter 1996) such as are discussed in this paper. Second, the proper motion in Table 1 is in good agreement with previous proper motion measurements (Rauch et al. 2004). With the revised distance, the tangential velocity is now increased to 88 km s^{-1} , the galactic orbit calculated from the proper motion and radial velocity will be altered, and the conclusion drawn by Rauch et al. about its origin in the thin disk may be changed.

The distance of RE1738+665 of 169_{-11}^{+13} pc is slightly closer than the 200 ± 35 pc derived spectroscopically (Barstow et al. 1994). This distance supports the gravity ($\log g = 7.8$) and mass ($\sim 0.62M_{\odot}$) of the central star (Barstow et al. 2003) being somewhat higher than most CSPN. A relatively high mass was proposed (Tweedy 1995) to account for its X-ray emission discovered in the Rosat survey. The emission was noted as unusual for such a hot, hydrogen-rich star, and is still unusual, despite the fact that the temperature derived now by Barstow et al. for RE1738+665 (and for other DA stars) is less extreme than considered by Tweedy.

The nature of PHL932 is problematic in several respects. First, we find a smaller parallax than measured by Hipparcos (see Sec. 2.3). The larger distance given in Table 3 helps resolve some of the discrepancy in $\log g$ for the central star between the observed gravity (Méndez et al. 1988) and the gravity deduced from the temperature and an assumed (normal) mass (Pottasch & Acker 1998). Nevertheless, the central star is a sdB star on the extended horizontal branch (Lisker et al. 2005), requiring extreme evolution to produce a PN. DeMarco et al. (2004) find the radial velocity is variable. One possibility is that the nebula is ionized ISM (Frew & Parker 2006), not a true PN. Alternatively, the true central star may be fainter and unresolved and not yet observed – with $M_V = 4.4$ for the sdB star in Table 3, a CSPN with a typical $M_V \sim 7$ could easily be hidden and only detectable at UV wavelengths. The radial velocity variations could be caused by the real CSPN, or there could be a more complicated triple system.

In observing nearby stars with accurate astrometry, it is sometimes possible to detect perturbations from an unresolved close companion with a period of the length of the observations or less, if such a companion exists. The USNO parallax program has discovered a number of such companions around nearby red dwarfs and white dwarfs. No perturbations are apparent for the 16 CSPN in this paper. These data rule out companions with periods less than 5–10 yr and with masses large enough to produce an apparent reflex motion of the central star of > 1 mas. In practice, early-M dwarf companions with these periods would be detected for these CSPN if they were present, and late-M companions would be detected for the closest of the sample. The data do not constrain the presence of companions with lower mass, such as from low-mass L or T dwarfs or planets.

4. FUTURE IMPROVEMENTS

Parallaxes from HST are likely to reach greater precision than the USNO ground-based results. However, limited HST observing time means that an extensive HST program for planetary nebulae parallaxes is unlikely to happen. Therefore, dramatic improvements beyond the ground-based program described here will have to wait until SIM or GAIA are in use.

Several other PNe are likely to be at distances where useful parallax measurements can be made now from the ground. As well as repeating a couple of the PNe in Table 3, it may be possible to get useful results for NGC 246, NGC 1360, NGC 1514, NGC 3242, PG0108+101, A35, A36, LT5, and Hu2-1. Some of these objects may be added to our program soon. Unfortunately, some of them have central stars (or companions to the central stars) sufficiently bright to require some change in the camera hardware in order to get higher dynamic range to reach faint reference stars. We hope other researchers will include some of these objects in their studies to compare distances determined with other methods. If other PNe are of particular importance and are likely to be at a distance closer than 500 pc, please contact us to request their addition to the program.

We thank the referee, Dr. H. Smith, for helpful comments and for suggesting adding Figure 4, as part of a thorough review. This research has made use of the SIMBAD database, operated at CDS, Strasbourg, France.

REFERENCES

- Acker, A., Fresneau, A., Pottasch, S.R., & Jasiewicz, G. 1998, *A&A*, 337, 253
- Barstow, M.A., Holberg, J.B., Marsh, M.C., Tweedy, R.W., Burleigh, M.R., Fleming, T.A., Koester, D., Penny, A.J., & Sansom, A.E. 1994, *MNRAS*, 271, 175
- Barstow, M.A., Good, S.A., Holberg, J.B., Hubeny, I., Bannister, N.P., Bruhweiler, F.C., Burleigh, M.R., & Napiwotzki, R. 2003, *MNRAS*, 341, 870
- Benedict, G.F., et al. 2003, *AJ*, 126, 2549
- Cahn, J.H., Kaler, J.B., & Stanghellini, L. 1992, *A&AS*, 94, 399
- Chu, Y.-H., Gruendl, R.A., Williams, R.M., Gull, T.R., & Werner, K. 2004, *AJ*, 128, 2357
- Ciardullo, R., Bond, H.E., Sipior, M.S., Fullton, L.K., Zhang, C.Y., & Schaefer, K.G. 1999, *AJ*, 118, 488
- Dahn, C.C., et al. 2002, *AJ*, 124, 1170
- Dahn, C.C., Behall, A.L., & Christy, J.W. 1973, *PASP*, 85, 224
- De Marco, O., Bond, H.E., Harmer, D., & Fleming, A.J. 2004, *ApJ*, 602, L93
- Frew, D.J., & Parker, Q. 2006, in *Proc. IAU Symp. 234, Planetary Nebulae in our Galaxy and Beyond*, ed. M.J. Barlow & R.H. Méndez (Cambridge: Cambridge University Press), in press
- Gutiérrez-Moreno, A., Anguita, C., Loyola, P., & Moreno, H. 1999, *PASP*, 111, 1163
- Hajian, A.R. 2006, in *Proc. IAU Symp. 234, Planetary Nebulae in our Galaxy and Beyond*, ed. M.J. Barlow & R.H. Méndez (Cambridge: Cambridge University Press), in press
- Harrington, R.S., & Dahn, C.C. 1980, *AJ*, 85, 454
- Harris, H.C., Dahn, C.C., Monet, D.G., & Pier, J.R. 1997, in *Proc. IAU Symp. 180, Planetary Nebulae*, ed. H.J. Habing & H.J.G.L.M Lamers (Dordrecht: Kluwer), 40
- Harris, H.C., et al. 2005, in *Astrometry in the Age of the Next Generation of Large Telescopes*, ASP Conf. Ser. 338, ed. P.K. Seidelmann & A.K.B. Monet (San Francisco: ASP), 122
- Hewett, P.C., Irwin, M.J., Skillman, E.D., Foltz, C.B., Willis, J.P., Warren, S.J., & Walton, N.A. 2003, *ApJ*, 599, L37

- Ishida, K., & Weinberger, R. 1987, A&A, 178, 227
- Landolt, A.U. 1992, AJ, 104, 340
- Lisker, T., Heber, U., Napiwotzki, R., Christlieb, N., Han, Z., Homeier, D., & Reimers, D. 2005, A&A, 430, 223
- Lutz, T.E., & Kelker, D.H. 1973, PASP, 85, 573
- Méndez, R.H., Groth, H.G., Husfeld, D., Kudritzki, R.-P., & Herrero, A. 1988, A&A, 197, L25
- Monet, D.G., Dahn, C.C., Vrba, F.J., Harris, H.C., Pier, J.R., Luginbuhl, C.B., & Ables, H.D. 1992, AJ, 103, 638
- Napiwotzki, R. 1999, A&A, 350, 101
- Napiwotzki, R. 2001, A&A, 367, 973
- Phillips, J.P. 2005, MNRAS, 357, 619
- Phillips, J.P. 2005, MNRAS, 362, 847
- Pier, J.R., Harris, H.C., Dahn, C.C., & Monet, D.G. 1993, in Proc. IAU Symp. 155, *Planetary Nebulae*, ed. R. Weinberger & A. Acker (Kluwer, Dordrecht), 175
- Pottasch, S.R. 1996, A&A, 307, 561
- Pottasch, S.R. & Acker, A. 1998, A&A, 329, L5
- Rauch, T., Kerber, F., & Pauli, E.-M. 2004, A&A, 417, 647
- Smith, H., Jr. 2003, MNRAS, 338, 891
- Terzian, Y. 1993, in Proc. IAU Symp. 155, *Planetary Nebulae*, ed. R. Weinberger & A. Acker (Kluwer, Dordrecht), 109
- Tweedy, R.W. 1995, Nature, 373, 666
- Tweedy, R.W., & Kwitter, K.B. 1996, ApJS, 107, 255
- Van de Steene, G.C., & Zijlstra, A.A. 1994, A&AS, 108, 485
- van Altena, W.F., Lee, J.T., & Hoffleit, E.D. 1995, *The General Catalogue of Trigonometric Stellar Parallaxes, Fourth Edition* (New Haven: Yale University Observatory)

Werner, K., Dreizler, S., & Wolff, B. 1995, *A&A*, 298, 567

Table 1. USNO Astrometric Data

Name	PN PN G	Number of Frames	Nights	Epoch	π_{rel} (mas)	$\Delta\pi$ (mas)	π_{abs} (mas)	μ_{rel} (mas yr ⁻¹)	PA (degrees)
TI800 CCD Program:									
NGC 6853	060.8–03.6	146	68	88.4–95.6	2.10 ± 0.38	0.53 ± 0.20	2.63 ± 0.43	14.2 ± 0.3	60.5 ± 2.5
NGC 6720	063.1+13.9	230	117	88.1–95.2	0.58 ± 0.45	0.84 ± 0.32	1.42 ± 0.55	9.0 ± 0.6	318.0 ± 3.3
A74	072.7–17.1	53	50	88.5–94.8	0.96 ± 0.62	0.37 ± 0.12	1.33 ± 0.63	1.8 ± 0.3	296.6 ± 7.6
Sh2-216	158.5+00.7	103	40	89.7–94.9	6.31 ± 0.88	1.06 ± 0.47	7.37 ± 1.00	23.8 ± 0.6	119.2 ± 1.5
PuWe1	158.9+17.8	61	31	87.9–95.8	2.58 ± 0.51	0.54 ± 0.24	3.12 ± 0.56	21.0 ± 0.3	186.9 ± 0.5
A21	205.1+14.2	66	53	87.9–95.8	1.60 ± 0.50	0.25 ± 0.10	1.85 ± 0.51	8.8 ± 0.5	204.0 ± 2.6
TEK2048 CCD Program:									
NGC 7293	036.1–57.1	228	169	92.6–02.6	3.64 ± 0.47	0.92 ± 0.12	4.56 ± 0.49	33.0 ± 0.1	86.7 ± 0.3
NGC 6853	060.8–03.6	264	178	97.4–02.7	3.21 ± 0.42	0.60 ± 0.20	3.81 ± 0.47	13.0 ± 0.2	61.0 ± 1.0
RE1738+665	096.9+32.0	204	137	97.3–03.5	5.16 ± 0.40	0.75 ± 0.12	5.91 ± 0.42	23.6 ± 0.1	130.4 ± 0.3
DeHt5	111.0+11.6	187	162	96.8–05.9	2.82 ± 0.54	0.52 ± 0.12	3.34 ± 0.56	21.4 ± 0.2	214.6 ± 0.5
PHL932	125.9–47.0	57	40	03.7–06.0	2.39 ± 0.61	0.97 ± 0.15	3.36 ± 0.62	37.8 ± 0.4	74.2 ± 0.8
HDW4	156.3+12.5	183	115	96.8–03.0	3.86 ± 0.35	0.92 ± 0.20	4.78 ± 0.40	24.4 ± 0.2	136.3 ± 0.4
Sh2-216	158.5+00.7	280	163	92.8–01.0	7.10 ± 0.24	0.71 ± 0.25	7.81 ± 0.35	23.5 ± 0.1	119.6 ± 0.2
PuWe1	158.9+17.8	249	122	92.8–01.0	1.97 ± 0.34	0.60 ± 0.15	2.57 ± 0.37	19.0 ± 0.2	184.2 ± 0.3
Ton320	191.4+33.1	153	136	96.9–06.2	1.23 ± 0.29	0.65 ± 0.15	1.88 ± 0.33	11.7 ± 0.1	203.5 ± 0.3
A7	215.5–30.8	172	155	93.9–03.0	0.88 ± 0.37	0.60 ± 0.23	1.48 ± 0.42	10.9 ± 0.1	304.5 ± 0.7
A24	217.1+14.7	90	86	96.8–05.9	1.45 ± 0.32	0.47 ± 0.10	1.92 ± 0.34	3.5 ± 0.1	265.2 ± 2.6
A31	219.1+31.2	135	95	96.9–03.0	0.83 ± 0.26	0.92 ± 0.20	1.76 ± 0.33	10.4 ± 0.1	226.5 ± 0.6
PG1034+001		24	24	04.0–06.2	3.68 ± 0.51	1.07 ± 0.15	4.75 ± 0.53	87.9 ± 0.5	293.3 ± 0.5

Table 2. Photometry of the Central Stars¹

Name	V	$B - V$	$V - I$	N
NGC 7293	13.525	-0.322	-0.415	2
NGC 6853	13.989	-0.298	-0.392	3
NGC 6720	15.749	-0.383	-0.299	2
A74	17.046	-0.334	-0.259	2
RE1738+665	14.580	-0.342	-0.339	3
DeHt5	15.474	-0.221	-0.166	2
PHL932	12.107	-0.254	-0.271	2
HDW4	16.528	-0.221	-0.236	1
Sh2-216	12.630	-0.295	-0.362	4
PuWe1	15.534	-0.244	-0.270	4
Ton320	15.702	-0.277	-0.408	2
A21	15.962	-0.293	-0.352	3
A7	15.479	-0.283	-0.330	2
A24	17.407	-0.285	-0.371	2
A31	15.519	-0.285	-0.314	2
PG1034+001	13.211	-0.299	-0.418	1

¹Johnson B and V , and Cousins I magnitudes.

Table 3. Results

PN	π_{abs} (mas)	Distance (1σ Range) (pc)	$E(B - V)$	M_V (1σ Range)	V_{tan} (km s ⁻¹)
NGC 7293	4.56 ± 0.49	219 (198–246)	0.03	6.73 (6.47–6.94)	34.2 ± 3.6
NGC 6853 ¹	2.64 ± 0.33	379 (337–433)	0.07	5.88 (5.59–6.14)	24.1 ± 3.2
NGC 6720	1.42 ± 0.55	704 (508–1149)	0.08	6.26 (5.20–6.97)	30.0 ± 13.7
A74	1.33 ± 0.63	752 (510–1428)	0.12	7.29 (5.90–8.14)	6.4 ± 4.0
RE1738+665	5.91 ± 0.42	169 (158–182)	0.05	8.29 (8.12–8.43)	18.9 ± 1.4
DeHt5 ²	3.34 ± 0.56	300 (256–360)	0.18	7.53 (7.13–7.87)	30.4 ± 5.3
PHL932 ²	3.36 ± 0.62	298 (251–365)	0.10	4.43 (3.99–4.80)	53.4 ± 10.2
HDW4	4.78 ± 0.40	209 (193–228)	0.16	9.43 (9.24–9.61)	24.2 ± 2.1
Sh2-216	7.76 ± 0.33	129 (124–135)	0.08	6.83 (6.73–6.92)	14.4 ± 0.6
PuWe1	2.74 ± 0.31	365 (328–412)	0.14	7.28 (7.02–7.52)	32.9 ± 3.8
Ton320	1.88 ± 0.33	532 (452–645)	0.07	6.86 (6.44–7.21)	29.5 ± 5.4
A21	1.85 ± 0.51	541 (424–746)	0.08	7.05 (6.35–7.58)	22.6 ± 6.7
A7	1.48 ± 0.42	676 (526–943)	0.10	6.02 (5.30–6.56)	34.9 ± 10.8
A24	1.92 ± 0.34	521 (442–633)	0.07	8.61 (8.16–8.97)	8.6 ± 1.6
A31	1.76 ± 0.33	568 (478–699)	0.07	6.53 (6.08–6.91)	28.0 ± 5.4
PG1034+001 ²	4.75 ± 0.53	211 (189–237)	0.05	6.43 (6.18–6.67)	87.9 ± 10.0

¹Parallax is a weighted mean of the two USNO measurements from Table 1 combined with the HST parallax from Benedict et al. (2003) (see Sec. 2.3).

²Results not final, observations continuing.

Table 4. Comparison with Other Studies

PN	Distance in pc:							
	This Paper	CKS ¹ 1992	TIW ² 1993	VZ ³ 1994	Zhang 1995	Pottasch 1996	Spectroscopic ⁴ 2001	Phillips 2005a
NGC 7293	219	157	160	400	420	280	290	290
NGC 6853	379	262	270	400	480	360	440	...
NGC 6720	704	872	840	1000	1130	500	1100	...
A74	752	...	230	850	1700	600
RE1738+665	169	200	200	...
DeHt5	300	...	400	350	510	510
PHL932	298	819	590	2340	3330	520	240	520
HDW4	209	350	250	250
Sh2-216	129	...	40	130	190	125
PuWe1	365	141	240	...	900	300	700	433
Ton320	532	...	≥500	350	350	...
A21	541	...	270	500	630	541
A7	676	216	220	...	700	550	700	700
A24	521	525	≥500	...	1900	600	...	286
A31	568	233	240	...	1010	400	1000	326
PG1034+001	211	155	...

¹Cahn *et al.* (1992)

²Terzian (1993), based on Ishida & Weinberger (1987)

³Van de Steene & Zijlstra (1994)

⁴Napiwotzki (2001); Napiwotzki (1999); Pottasch (1996) Table 6

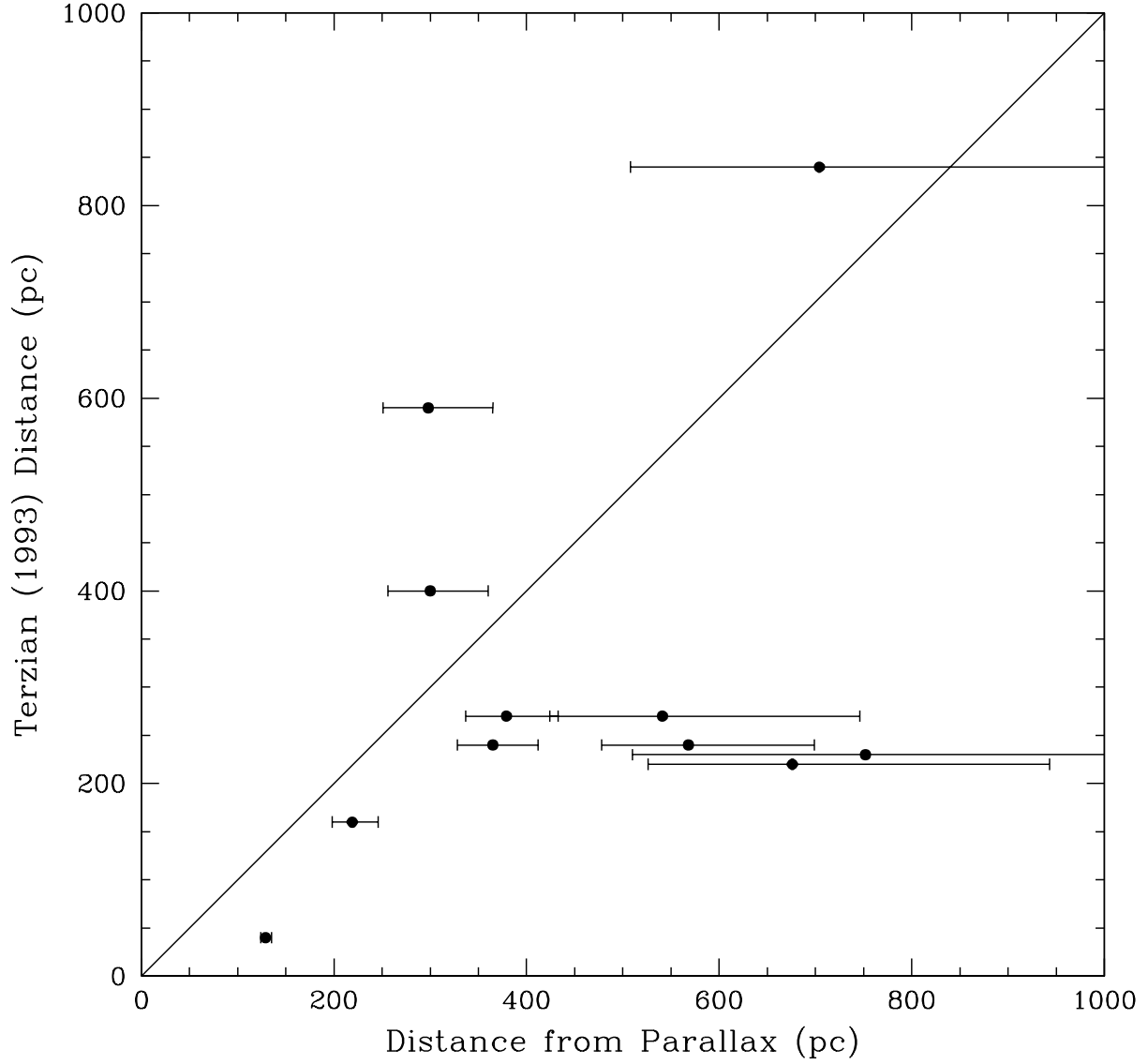


Fig. 1.— Distances of nearby PNe tabulated by Terzian (1993; his Table 3) and his primary source (Ishida & Weinberger 1987) compared with this paper.

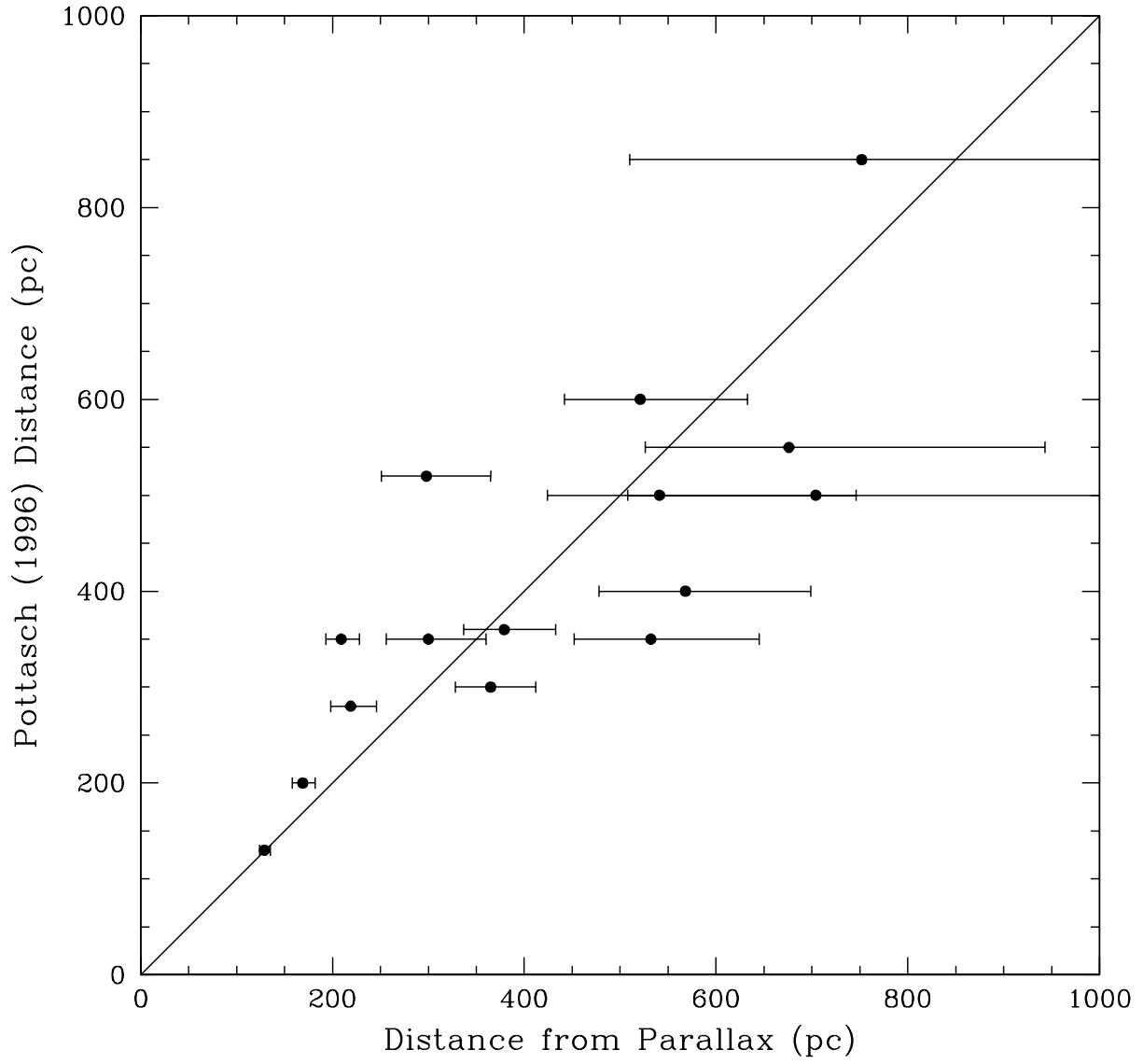


Fig. 2.— Distances of PNe from Pottasch (1996; his Table 9) compared with this paper.

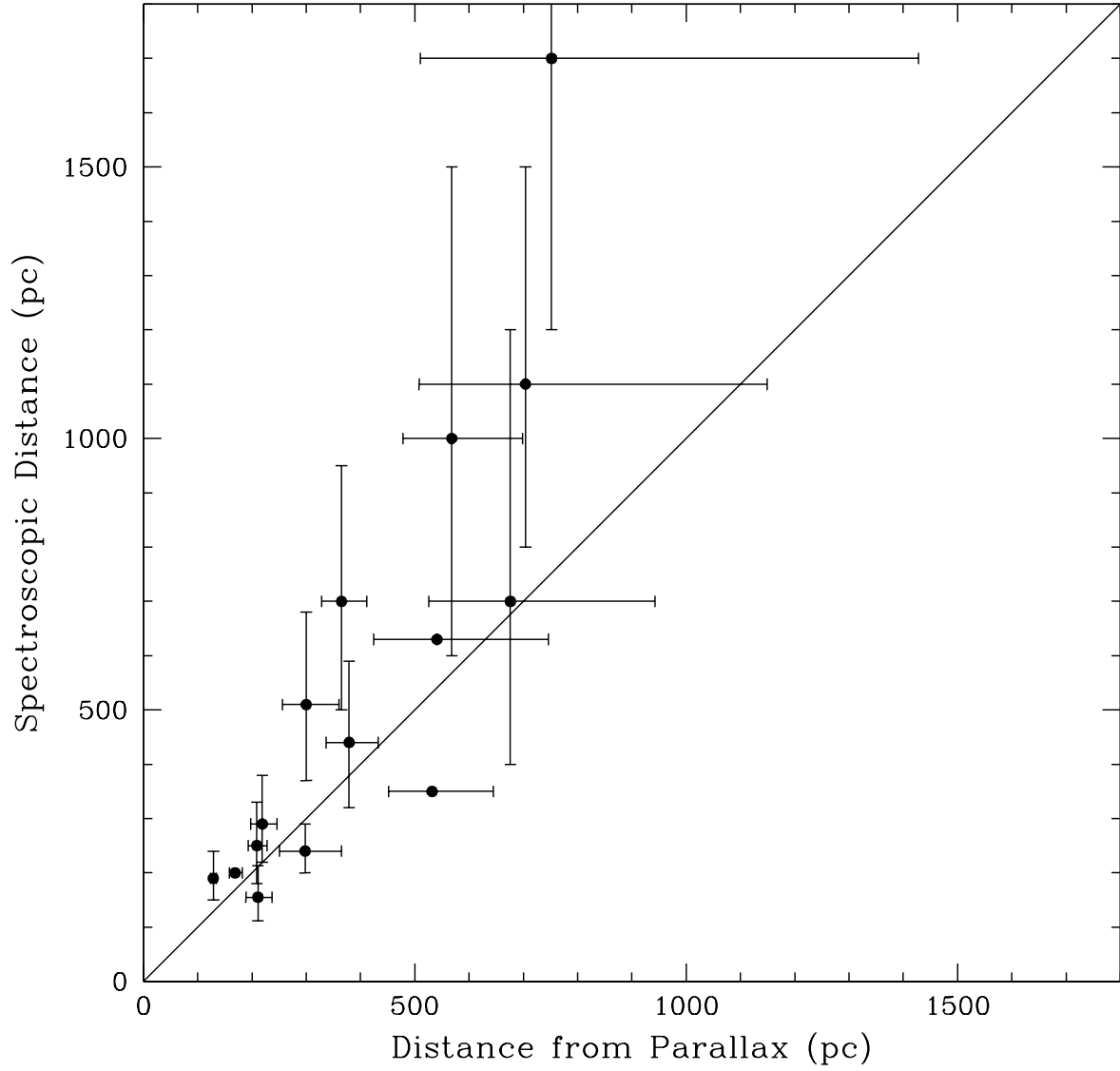


Fig. 3.— Distances of PNe from spectroscopic analysis of Napiwotzki (1999; 2001) plus two objects from Pottasch (1996; his Table 6) with spectroscopic (“gravity”) distances compared with this paper.

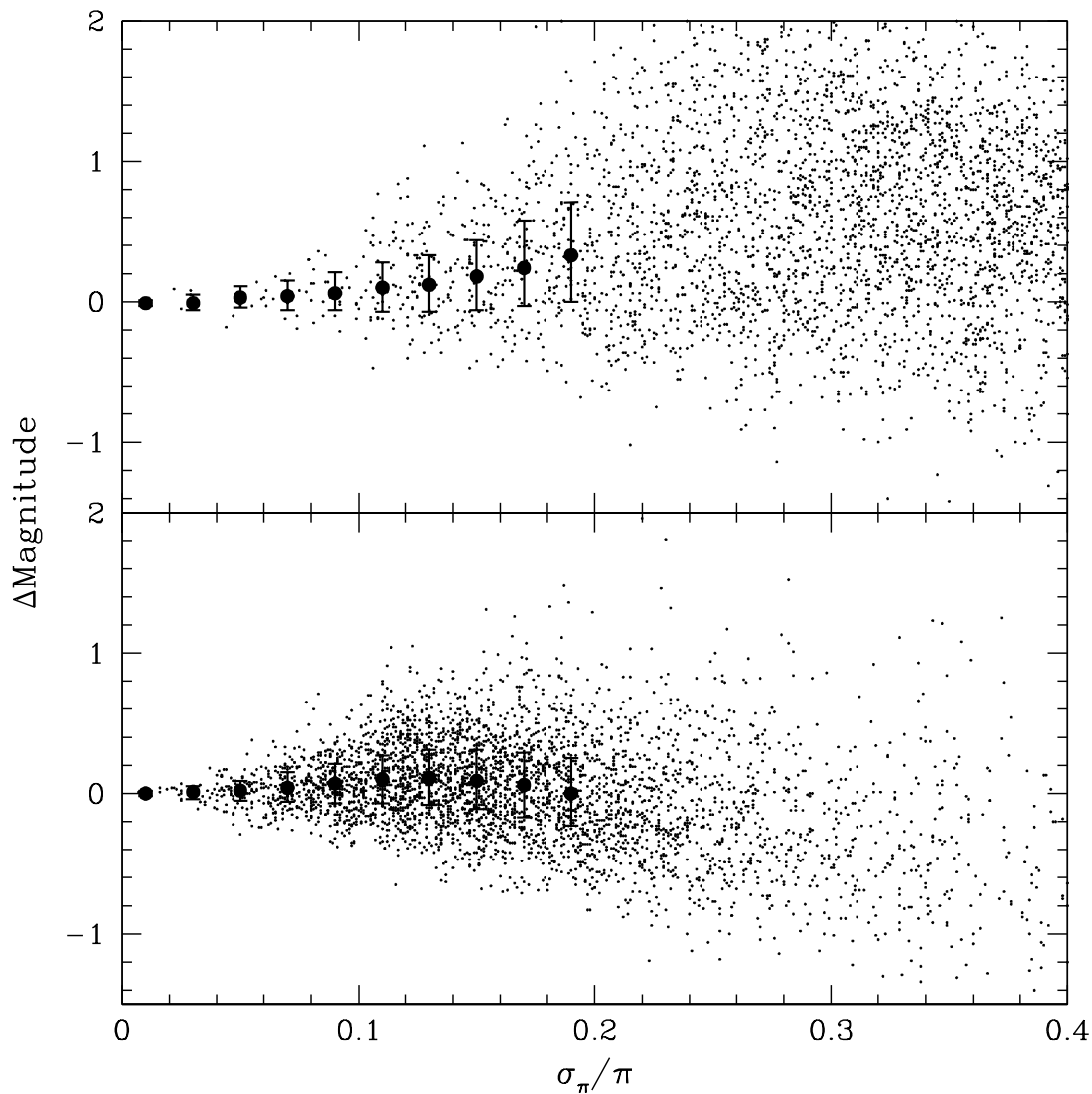


Fig. 4.— The bias in distances determined from parallaxes for a model disk population, expressed here as a bias in absolute magnitudes. The top panel shows the bias for a disk population – it is *not* representative of the sample in this paper. The lower panel includes a sample selection for objects believed in advance to be nearby. This panel is an attempt to model the sample in this paper realistically.